Journal of Alloys and Compounds 504S (2010) S323–S327

Contents lists available at ScienceDirect

Journal of Alloys and Compounds

journal homepage: www.elsevier.com/locate/jallcom

Spark plasma sintering and hot isostatic pressing of nickel nanopowders elaborated by a modified polyol process and their microstructure, magnetic and mechanical characterization

M.A. Bousnina [a,b], A. dakhlaoui Omrani [b,c,*], F. Schoenstein [b], P. Madec [b], H. Haddadi [b], L.S. Smiri [a], N. Jouini [b]

[a] Unité de recherche 99/UR12-30, Département de Chimie, Faculté des Sciences de Bizerte, 7021 Jarzouna, Tunisia
[b] Laboratoire des Propriétés Mécaniques et Thermodynamiques des Matériaux, LPMTM, CNRS UPR 9001 Université Paris XIII, 99 Avenue J.B. Clément, 93430 Villetaneuse, France
[c] Laboratoire de Physique et Chimie des Nano-Objets, INSA de Toulouse, 135 Avenue de Rangueil, 31077 Toulouse cedex 4, France

ARTICLE INFO

Article history:
Received 5 July 2009
Received in revised form 9 February 2010
Accepted 19 February 2010
Available online 3 March 2010

Keywords:
Nanostructured nickel materials
Sintering
Mechanical properties
Magnetic measurements

ABSTRACT

The microstructure, magnetic and mechanical properties of spark plasma sintered (SPS) and hot isostatic pressed (HIP) nickel nanopowders are investigated. The microstructure study shows that the increase in the particle size was more limited when consolidation was performed by the SPS than by the HIP process. The grain size is in the range 0.17–0.2 μm in the case of the SPS consolidated sample while it is in the range 0.4–0.62 μm in the case of the HIPed sample. The ratio of the yield stress in the HIP and SPS consolidated samples to the yield stress in the bulk nickel sample is greater than two and three times, respectively. Vickers microhardness measurements give the same ratios. A ferromagnetic behaviour was deduced from the magnetic characterizations of the as-prepared nickel powder as well as the consolidated samples.

1. Introduction

In the last few years, considerable effort has been devoted to the design and controlled fabrication of dense nanostructured materials of the 3d elements for their unusual properties especially in the mechanical and physical fields [1–5]. Up to now a variety of elaboration methods have been used. They adopt either the "Top-down" or the "Bottom-Up" processes. In the former process the coarse-grained materials are refined into nanostructured powders by severe plastic deformation (SPD) techniques such as equal-channel angular pressing (ECAP), high-pressure torsion (HPT) and repeated cold-rolling and folding (F&R) [6–8]. While the "Bottom-Up" process consists in two steps: (i) synthesis of nanoparticles and (ii) consolidation by various processes such as hot isostatic pressing (HIP) [9], spark plasma sintering (SPS) [10] and pulse electric current sintering (PECS) [11]. Here we report on the elaboration of dense nanostructured nickel samples using the Bottom-Up strategy: first the nanopowder was synthesized by the well known polyol process, modified using the sodium hypophosphite as reducing agent, and then the densification of the powder was performed by the HIP and SPS processes. The polyol process has been used for its several advantages particularly as complexant and as a surfactant agent which adsorbs on the surface of the elementary particles preventing their agglomeration [12]. To achieve consolidation, HIP and SPS have been used to make it possible to apply high pressure in the former which is likely to favour elaboration of full dense nanostructured material and the advantage of a short cycle time of consolidation in the latter process which permits consolidation of powder with a limited grain growth.

The microstructure, mechanical and magnetic behaviours of the elaborated dense materials were reported and discussed as a function of the consolidation process.

2. Experimental

2.1. Synthesis of the powder

The Ni nanopowder has been prepared according to the following procedure: the appropriate amount of nickel (II) acetate tetrahydrate ($Ni(OAc)_2{\cdot}4H_2O$) (0.08 M), sodium hydroxide (NaOH) (0.2 M) and anhydrous sodium hypophosphite (NaH_2PO_2) (0.24 M) were mixed together, stirred at room temperature until complete dissolution in ethyleneglycol (EG), then heated to the boiling temperature of the liquid. The water coming from metal acetate was distilled off and the reaction was left to proceed for two hours. Then, the black precipitate was collected by centrifugation, washed several times with ethanol and acetone then dried in an oven at 50 °C.

* Corresponding author at: Laboratoire des Propriétés Mécaniques et Thermodynamiques des Matériaux, LPMTM, CNRS UPR 9001 Université Paris XIII, 99 Avenue J.B. Clément, 93430 Villetaneuse, France. Tel.: +33149403494; fax: +33149403938.
E-mail address: dakhlaoui_amel@yahoo.Fr (A. dakhlaoui Omrani).

0925-8388/$ – see front matter © 2010 Elsevier B.V. All rights reserved.
doi:10.1016/j.jallcom.2010.02.142

2.2. Consolidation of the powder

Before being consolidated the nickel powder was initially heated under hydrogen at 300 °C for one hour to clear it of organic impurities and to thermally reduce all trace of nickel oxides probably present on the surface of the particles.

To be consolidated using the hot isostatic pressure process, the powder was placed in a cylindrical stainless steel capsule then pumped for about one week to extricate the residual air. After being closed, the capsule was first isostatically pressured through argon up to 120 MPa then heated up to 650 °C and holding for one hour then the hipping process was switched off. Spark plasma sintering of the powder was achieved using the following process: after establishing a primary vacuum and passing an argon flow into the apparatus, an uniaxial pressure was firstly applied to the graphite die containing the powder. Its value was increased up to 53 MPa after 1 min and then the heating started while maintaining this pressure. The final holding temperature is between 598 °C and 600 °C and it was maintained for 5 min. It should be mentioned that the pressure and the temperature of consolidation with the SPS process have been fixed on the basis of the HIP densification observation: in fact from the diagram powder's consolidation evolution using the HIP process, it has been observed that the displacement of the capsule was stabilized, and consequently the consolidation was achieved, at a temperature of approximately 560 °C and a pressure far lower than 120 MPa and so we have chosen to perform the SPS tests at 600 °C and a pressure of 53 MPa.

2.3. Characterization techniques

The X-ray diffraction patterns were collected on an INEL diffractometer with a cobalt anticathode ($\lambda = 1.7809$ Å). The size and morphology of the particles and the microstructure of the consolidated samples were studied using a JEOL-2011 transmission electron microscope (TEM) operating at 200 kV. HIP experiments were realized with a hot isostatic pressing apparatus equipped with a dilatometer allowing in situ control of the consolidation process [13]. SPS consolidation of the powders was accomplished with a spark plasma sintering (SPS)-515S SYNTEX apparatus. The mechanical properties were studied on parallepedic samples in uniaxial compression at a strain rate of $2 \times 10^{-4}\ s^{-1}$ at room temperature using an Instron universal machine (model 1195) with a load cell of 100 kN maximum capacity. The compressive mechanical (elastic plus plastic) strain was determined from the absolute magnitude Δl of change in specimen length as $\varepsilon = -\ln(l/l_0) = -\ln((l_0 - \Delta l)/l_0)$. Microhardness measurements were conducted on the plane perpendicular to the pressing direction using a Duramin 20 Vickers device under a test force of 1.916 N for 5 s.

The variation of the magnetization as a function of the applied magnetic field was recorded at 5 K with a superconducting quantum interference device (SQUID) magnetometer model MPMS-SS.

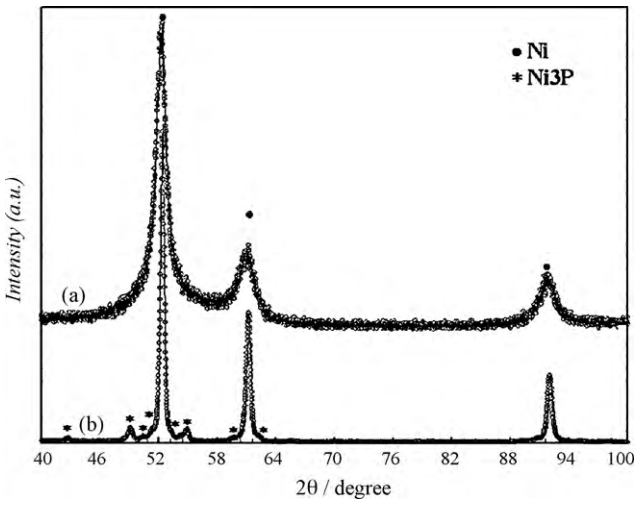

Fig. 1. XRD patterns of as-elaborated Ni powder (a) and dense samples (b).

3. Result and discussion

3.1. X-ray diffraction characterization

X-ray diffraction patterns of the dense samples (Ni_{HIP} and Ni_{SPS}) (Fig. 1b) show the presence of nickel phosphide (Ni_3P) phase while no trace of it was observed in the pattern of the powder (Fig. 1a). From a peak intensity analysis, using Match program [14], the percentage of this impurity was estimated at 8% and 6% for the Ni_{HIP} and Ni_{SPS} samples, respectively. The broadening of the diffraction lines of the consolidated samples decreases in comparison with those of the precursor powder which indicates an increase in the crystallites' size. The calculation of the average crystallites' size based on the width of the $2\theta = 44.42°$ diffraction peak by Scher-

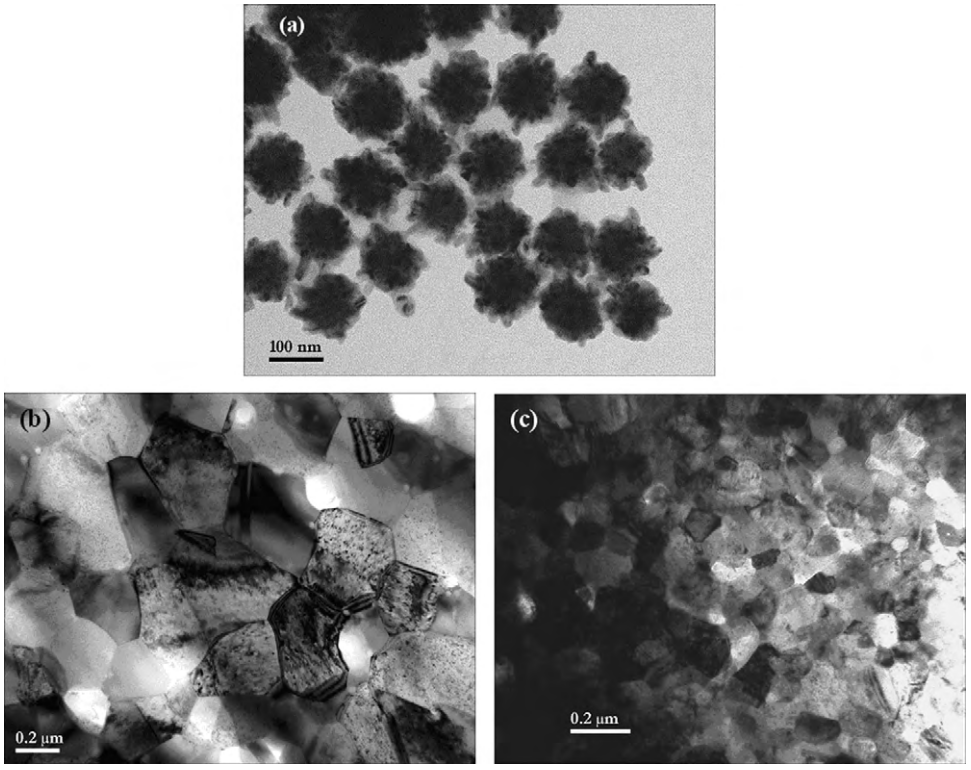

Fig. 2. TEM micrographs of the as-elaborated Ni precursor powder (a) the Ni_{HIP} sample (b) and the Ni_{SPS} sample (c).

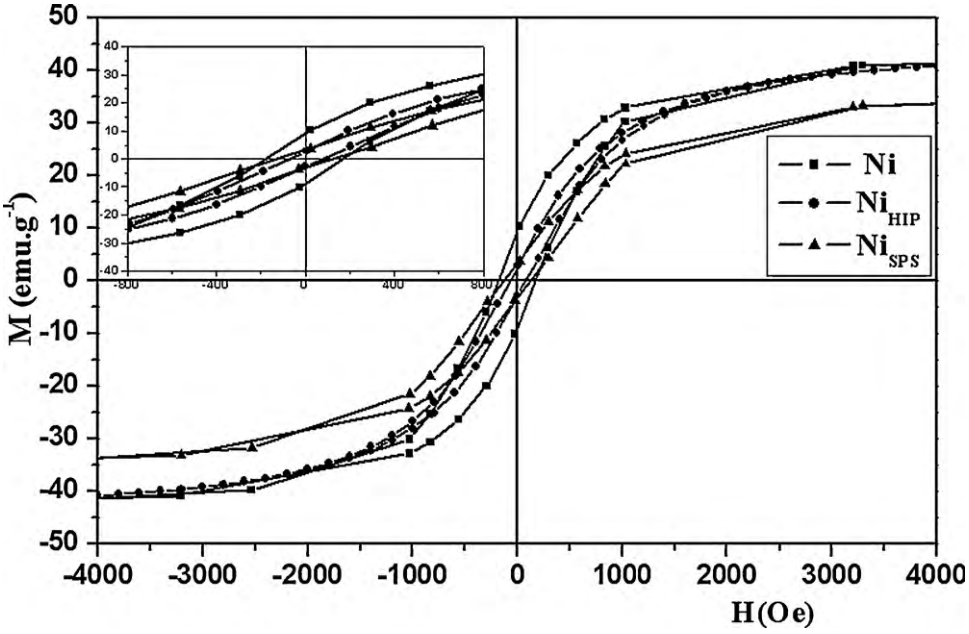

Fig. 3. Variation of magnetization of Ni powder, Ni_{HIP} and Ni_{SPS} samples with the applied magnetic field at 5 K.

rer's formula gives values of 11 nm, 44 nm and 42 nm, respectively for the powder, the Ni_{HIP} and the Ni_{SPS}.

3.2. TEM characterization

The TEM micrograph of the powder shows particles with a spherical morphology and roughly 100 nm in diameter (Fig. 2a). The difference between the particles' diameter given by the TEM and the crystallites' size calculated on the basis of the X-ray pattern suggests that the Ni particles are formed through an aggregation growth process rather than an Ostwald repining process. For the consolidated samples (Fig. 2b and c), it can be clearly observed that both HIP and SPS consolidation processes induce no significant change of the particles' morphology but an increase in the grains' size could be clearly noted. The grains' diameter increased up to 0.62 μm in the case of the former sample and 0.2 μm in the case of the second which clearly indicates that the SPS process limits the grain growth during sintering. No evidence of presence of residual porosity could be deduced from the TEM micrographs, although the relative densities of the two samples (88% for Ni_{HIP} and 86% for Ni_{SPS}) are lower than that of the bulk nickel which suggests that the presence of the Ni_3P impurity in the dense material could be the origin of this difference.

3.3. Magnetic characterization

Hysteresis loops of the powder and the dense samples (Fig. 3) show a ferromagnetic behaviour for the three samples. As can be seen, the H_c values of the dense samples (85 Oe for Ni_{HIP} and 111 Oe for the Ni_{SPS}) are close to that of the bulk nickel (100 Oe) [15] while a clear improvement is observed in the powder (175 Oe). The slight anisotropic morphology and the small size of the nanoparticles of the Ni powder could be the origin of its higher coercivity. The increase of the particles' size during sintering and the strong particle–particle interaction could be the origin of the decrease in the coercivities of the dense samples.

The saturation magnetization (M_s) of the nanoparticles ($\approx$41 emu g^{-1}) as well as those of the consolidated samples ($\approx$40 emu g^{-1} for the Ni_{HIP} and 35 emu g^{-1} for Ni_{SPS}) were slightly reduced compared to that of the bulk nickel (55 emu g^{-1}) [15] which is probably due to the surface oxidation of the particles that reduces the effective magnetic moment [16].

3.4. Mechanical behaviour

The main mechanical characteristics of the consolidated samples Ni_{HIP} and Ni_{SPS} as well as that of bulk commercially obtained nickel (Ni_{Bulk}) are summarized in Table 1. Their true stress *vs.* true strain curves are given in Fig. 4. The Ni_{Bulk} sample shows the lowest yield stress (510 MPa) and the greatest ductility (more than 10%). No hardening occurred during straining and a large plateau is observed on the stress–strain curve.

The value of the yield stress of the Ni_{HIP} sample is more than two times greater (1160 MPa). It exhibits a low ductility about 3% and a weak hardening. Despite these two observations, the failure process of this sample seems to be ductile. It is evidenced by elongated dimples [17,18] observed at various places on the fracture surface (Fig. 5a). This difference between the mean value of ductility and the local observations can be explained by shear band localisation before the fracture occurs. In this case the reached strains can justify SEM observations.

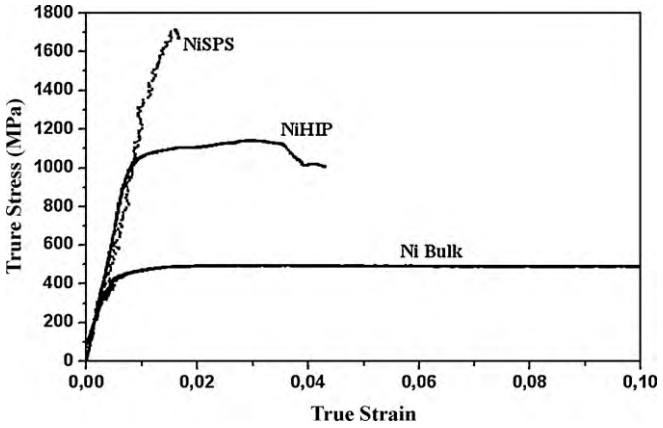

Fig. 4. Typical tensile stress–strain curve for Ni_{HIP}, Ni_{SPS} and bulk samples.

Table 1
Grain sizes and main mechanical characteristics of the Ni sintered samples and Ni bulk.

Sample	Grain size (nm)	Density (relative density)	Maximum strength (MPa)	Hardness (Vickers)
Ni_{HIP}	400–620	7.822 (87.9%)	1160	306
Ni_{SPS}	0.17–0.2	7.56 (86%)	1730	680
Ni Bulk		8.89 (99.98%)	510	184

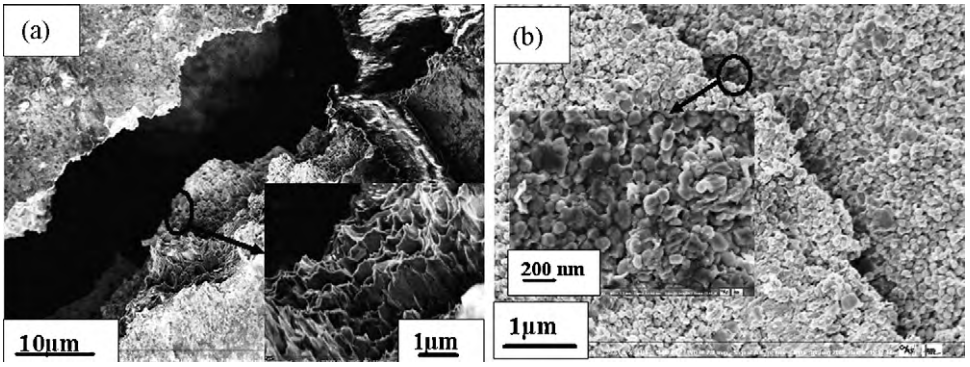

Fig. 5. SEM micrograph of fracture surface of the Ni_{HIP} sample (a) and the Ni_{SPS} sample (b). Inset of the two figures are the selected zones with higher magnification.

Concerning the Ni_{SPS} sample, its yield stress (1730 MPa) is three times higher than the yield stress of the Ni_{Bulk} sample. Fracture occurred during elastic regime and it could be clearly observed on the fracture surface (Fig. 5b) that the Ni_{SPS} sample exhibits a brittle fracture. The analysis of the Ni_{SPS} sample provided clear evidence that inter-particle de-cohesion had occurred during fracture and that the nanoparticles of nickel remain spherical since no plastic deformation occurred either during elaboration or during mechanical loading. This fact could explain the poor ductility of this sample.

Vickers microhardness measurements give the same tendency as the uniaxial compression tests: the Vickers hardness of the Ni_{Bulk} sample was measured as 184 HV while the Ni_{HIP} and Ni_{SPS} samples show significantly higher hardness: 306 HV and 680 HV, respectively. This result confirms that the SPS sintered sample is stronger than the HIPed sample which could be a consequence of its smaller grain size.

All these results concord with the enhancement of strength as the grain size decreases [19–21]. A similar behaviour of Ni, Cu, and Fe nanostructured materials has been reported earlier [19–22]. However, it should be noted that the great strength of the as-elaborated dense materials is accompanied by a significant decrease in the ductility especially as concerns the Ni_{SPS} samples which fail at the elastic stage.

The ductility of the Ni_{SPS} can be increased if the particles' cohesion is improved without increasing the size of grains. There is a competition between two phenomena: (i) the first is the de-cohesion which occurs in the elastic domain when the particles are very small (less than 200 nm), (ii) and the second phenomenon is the plastic deformation where the yield stress increases when the size of grains decreases.

4. Conclusion

In a first stage, nickel nanoparticles have been elaborated by a modified polyol process. They present a spherical morphology with approximately 100 nm in diameter. In a second stage these nanoparticles have been consolidated by spark plasma sintering and hot isostatic pressure. A more limited increase of the particle size is observed in the case of the sample consolidated using the SPS process than the hot isostatic pressed process. Density measurement gives comparative values but lower than that of the bulk sample. XRD patterns of the sintered samples show the presence of Ni_3P as impurity which could contribute to the decrease in the density value.

The magnetic measurements indicate a ferromagnetic behaviour in the precursor powder as well as of the consolidated samples. Mechanical measurements show a real increase in the yield stress that is accompanied by a poor ductility.

Investigations are currently conducted in order to obtain nanostructured nickel with a good compromise between high saturation magnetization, high strength combined with acceptable ductility. The main factors investigated are the starting size of the nanoparticles and the consolidation parameters (temperature, pressure and time).

Acknowledgements

A. Dakhlaoui Omrani highly acknowledges the financial support of the IDB (Islamic Development BANK). We thank J. Morrice-Abrioux from IUT Saint-Denis, Université Paris 13 for her help to improve the English expression of the manuscript.

References

[1] H. Gleiter, Nanostruct. Mater. 6 (1995) 3.
[2] Y. Nakamoto, M. Yuasa, Y. Chen, H. Kusuda, M. Mabuchi, Scripta Mater. 58 (2008) 731.
[3] A. Kulovits, S.X. Mao, J.M.K. Wiezorek, Acta Mater. 56 (2008) 4836.
[4] A.A. Karimpoor, U. Erb, K.T. Aust, G. Palumbo, Scripta Mater. 49 (2003) 651.
[5] F. Ebrahimi, G.R. Bourne, M.S. Kelly, T.E. Matthews, Nanostruct. Mater. 11 (3) (1999) 343.
[6] A. Dubravina, M.J. Zehetbauer, E. Schafler, I.V. Alexandrov, Mater. Sci. Eng. A 387–389 (2004) 817.
[7] R.Z. Valiev, M.J. Zehetbauer, Y. Estrin, H.W. Höppel, Y. Ivanisenko, H. Hahn, G. Wilde, H.J. Roven, X. Sauvage, T.G. Langdon, Adv. Eng. Mater. 9 (7) (2007) 527.
[8] G.P. Dinda, H. Rösner, G. Wilde, Mater. Sci. Eng. A 410–411 (2005) 328.
[9] S. Billard, J.P. Fondère, B. Bacroix, G.F. Dirras, Acta Mater. 54 (2006) 411.
[10] B.-N. Kim, K. Hiraga, K. Morita, H. Yoshida, Scripta Mater. 57 (2007) 607.
[11] Y. Zhou, K. Hirao, Y. Yamauchi, S. Kanzaki, J. Eur. Ceram. Soc. 24 (2004) 3465.
[12] L. Poul, S. Ammar, N. Jouini, F. Fiévet, J. Sol–Gel Sci. Technol. 26 (2003) 261.
[13] C. Rizkallah, J.P. Fondère, H.F. Ryanaud, A. Vignes, Rev. Métallurgie-CIT/Science et Génie des Matériaux 12 (2001) 1109.
[14] K. Brandenburg, H. Putz, Match: Phase identification from powder diffraction, (C) 2003–2009 Crystal IMPACT.

[15] X. Ni, Q. Zhao, H. Zheng, B. Li, J. Song, D. Zhang, X. Zhang, Eur. J. Inorg. Chem. 23 (2005) 4788.
[16] X. Ni, Y. Zhang, J. Song, H. Zhen, J. Crys. Growth 299 (2007) 365 (and references there in).
[17] M.A. Mayers, A. Mishra, D.J. Benson, Prog. Mater. Sci. 51 (2006) 427.
[18] X. Shen, J. Lian, Z. Jiang, Q. Jiang, Mater. Sci. Eng. A 487 (2008) 410.
[19] E.O. Hall, Proc. Phys. Soc. Lond. Sect. B 64 (1951) 747.
[20] W.Q. Cao, G.F. Dirras, M. Benyoucef, B. Bacroix, Mater. Sci. Eng. A 462 (2007) 100.
[21] D. Jia, K.T. Ramesh, E. Ma, Acta Mater. 51 (2003) 3495.
[22] J. Gubicza, H.-Q. Bui, F. Fellah, N. Szász1, G. Dirras, Mater. Sci. Forum 589 (2008) 93.